



Ng, KH., Tameh, EK., & Nix, AR. (2005). A new hybrid geometrical optics and radiance based scattering model for ray tracing applications. In *International Conference on Communications, 2005 (ICC 2005)* (Vol. 4, pp. 2168 - 2172). Institute of Electrical and Electronics Engineers (IEEE).
<https://doi.org/10.1109/ICC.2005.1494721>

Peer reviewed version

Link to published version (if available):
[10.1109/ICC.2005.1494721](https://doi.org/10.1109/ICC.2005.1494721)

[Link to publication record on the Bristol Research Portal](#)
PDF-document

University of Bristol – Bristol Research Portal

General rights

This document is made available in accordance with publisher policies. Please cite only the published version using the reference above. Full terms of use are available:
<http://www.bristol.ac.uk/red/research-policy/pure/user-guides/brp-terms/>

A New Hybrid Geometrical Optics and Radiance Based Scattering Model for Ray Tracing Applications

K. H. Ng, E.K.Tameh, A.R. Nix
Centre for Communications Research
Merchant Venturers Building, Woodland Road,
University of Bristol, Bristol, UK
k.h.ng@bris.ac.uk, tek.tameh@bris.ac.uk, andy.nix@bris.ac.uk

Abstract— This paper presents a new hybrid geometrical optics (GO) and radiance based rough surface scattering model for use in ray tracing propagation models. The reflectance model includes the effects of both specular and diffuse reflection. The specular component is modelled using GO Fresnel reflections, while the diffuse components are modelled using radiance reflectance. The hybrid scattering model is then developed and implemented within an existing three-dimensional microcellular ray tracing model. Comparisons of predicted path loss and rms delay spread are made at 1.92 GHz using site specific measurements in an urban environment. The results demonstrate that scattering can be an important mechanism at this frequency. Significant improvements in prediction accuracy are demonstrated with the new hybrid scattering model.

Keywords— ray tracing, scattering, radiance, propagation

I. INTRODUCTION

The high frequency approximation of radio wave propagation using geometric optics (GO) has enabled the development of many site-specific deterministic propagation models [1]-[3]. These models have shown good prediction agreement with measurement data. GO based propagation models use a ray tracing approach to identify all possible ray paths in the environment (up to a certain order). These ray paths encapsulate various major propagation mechanisms, such as transmission, scattering and diffraction. Although simple transmission and diffraction can be modelled with reasonable accuracy using the popular GO Fresnel and Uniform Theory of Diffraction (UTD) models [4]-[5], the scattering of electromagnetic (EM) waves from rough surfaces is more difficult to quantify and normally absent in prediction models.

The scattering of EM waves from rough surfaces can be classified into two components, 1) specular reflection and 2) diffuse reflection. Specular reflection follows the law of reflection (Snell's Law); however this does not apply for the diffuse component [6]. The scattered energy contained in each component depends on the surface roughness. Smooth surfaces result almost entirely in specular reflection, while rough surfaces generate strong diffuse components. One popular guideline for characterizing the surface roughness is the Rayleigh criterion [6], which states that a surface is

smooth if:

$$h < \frac{\lambda}{8 \sin(\gamma)} \quad (1)$$

where h represents the height difference of the surface irregularities, γ is the grazing angle of incident, and λ is the carrier wavelength.

In conventional GO based ray tracing models [1]-[3], scattering from surfaces is generally assumed to be specular and the diffuse reflection is omitted. Specular reflection is commonly modelled using the GO Fresnel reflection coefficients, which are augmented with a roughness attenuation factor [5]. In a real-world environment, most surfaces cannot be considered to be smooth at high carrier frequencies (>1 GHz). Furthermore, surfaces in these models are usually approximated by single planes, while in reality the underlying surface irregularities can be quite significant. Diffuse reflection in these cases may contribute significantly to the received power.

In order to supplement specular reflection in conventional propagation models, numerous models have been developed in the literature to include the effects of diffuse reflection [7]-[10]. These scattering models often rely on radar and radiosity techniques [11], [12]. In these models, each surface plane is represented by many small facets. Channel multipath components are then modelled by the incoherent sum of energy transfer links between each facet. UTD models can be applied between these links to support edge diffractions [10]. The main drawback of these models is computational cost, which is considerably greater than the GO based ray tracing model for the same order of reflection. Greater complexity occurs since reflections (specular or diffuse) in the scattering models occur at each facet, whereas reflections (specular) in the ray tracing models occur at each surface plane.

Although ray tracing techniques have been used extensively in propagation modelling, radiosity/radiance techniques have only been adopted in recent years. Both radiosity and ray tracing concepts have long been established in the computer graphics industry. Both methods have their own advantages and their convergence has already led to benefits in computer graphics applications [13]. A similar concept can be applied to

propagation modelling. In [9], a combined ray tracing model was presented based on Vertical Plane Launching (VPL) and radiosity scatter modelling. The work demonstrated that in combination, more accurate predictions were obtained. However, it is not clear whether this combined model satisfies the EM conservation of energy. In this paper, a hybrid scattering model is developed that supplements conventional ray tracing with the addition of diffuse reflection. The model extends the work of [9] and takes proper consideration of the EM validity. Because of this, the calculation of diffuse reflection can be treated in a similar manner to specular reflection in conventional ray tracing. As such, our hybrid scattering model can be easily applied to any conventional GO based ray tracing model to include the effects of rough surface scattering.

II. HYBRID GO AND RADIANCE BASED REFLECTANCE MODEL

The new hybrid GO and radiance based scattering model represents the specular reflection using the GO Fresnel reflection technique and the diffuse reflection using the radiance diffuse reflectance method. Radiance of a surface is defined as the total radiant flux per unit solid angle per unit projected surface area. Radiance model is often expressed in term of BRDF (Bidirectional Reflectance Distribution Function), which represents the ratio of the reflected radiance to the incident flux per unit area. Hence, in terms of radiance, the following equation can be written:

$$L_r = \begin{cases} P_0 \left(\frac{p_s R^2}{dA \cos(\theta_r)} + p_d f_{dr} \cos(\theta_i) \right) & \text{if } \theta_i = \theta_r, \\ P_0 (p_d f_{dr} \cos(\theta_i)) & \text{otherwise} \end{cases} \quad \text{if } \begin{cases} \phi_r = \pi - \phi_i \\ \text{otherwise} \end{cases} \quad (2)$$

The BRDF can be expressed as:

$$f_r = \begin{cases} p_s R^2 + p_d f_{dr} & \text{if } \theta_i = \theta_r, \phi_r = \pi - \phi_i \\ p_d f_{dr} & \text{otherwise} \end{cases} \quad (3)$$

where R is the Fresnel reflection coefficient; f_{dr} is the diffuse BRDF model with albedo $\rho = R^2$; θ_r is the reflection angle between the surface normal and the reflected direction; dA is the reflection surface area; p_s is the fraction of the albedo used for specular reflection and p_d is the fraction of the albedo used for diffuse reflection, such that $(p_s + p_d) \leq 1$; p_s is given by the rough surface attenuation factor of [6].

The balance of the reflected energy between the specular and diffuse components is controlled by p_s and p_d . The relationship between the definitions of radiance and BRDF in the new reflectance model may not be consistent with conventional definitions. This is due to the delta function in the specular component, since now the specular reflection only occurs when the law of reflection is satisfied [4]. Nevertheless, these definitions are still justified in accordance to the standard definitions.

In order to use radiance model in EM applications, it is necessary for the model to conform to two fundamental EM

laws, i.e. the conservation of energy and Helmholtz's reciprocity. The conservation of energy law states that the ratio of the total exiting energy over the incident energy on a surface area has to be smaller than unity. For most radiance models, this would require [12]:

$$\int_{\Omega} f_r \cos(\theta_r) d\omega_r \leq 1 \quad (8)$$

Helmholtz reciprocity states that the power transfer in one direction must be equal to the power transfer in the opposite direction. Most plausible BRDF models satisfy these laws.

In order to ensure that the new hybrid model satisfies both fundamental EM laws, the BRDF chosen for the diffuse reflection component (f_{dr}) must be plausible. Suitable functions include the Lambertian and Oren models [14]. Given the better accuracy and realism of the Oren model, this approach was selected for use in our hybrid scattering model. The simplified Oren model is given as [14]:

$$f_{dr} = \frac{\rho}{\pi} (A + B.K) \quad (4)$$

$$K = \text{Max}[0, \cos(\phi_r - \phi_i)] \sin(\text{Max}[\theta_i, \theta_r]) \tan(\text{Min}[\theta_i, \theta_r]) \quad (5)$$

$$A = 1.0 - 0.5 \frac{\sigma^2}{\sigma^2 + 0.33} \quad (6)$$

$$B = 0.45 \frac{\sigma^2}{\sigma^2 + 0.09} \quad (7)$$

where σ denotes the standard deviation of the slope angle of the micro-facets for the surface, which is used to describe the degree of roughness. Assuming the maximum of A is 1 and $K = \cos(\phi_r - \phi_i) \sin \theta_r \tan \theta_r$; the ratio of the total reflected energy density to the incident energy density R_p is given as:

$$\begin{aligned} R_p &= \int_{\Omega} p_s R^2 + p_d f_{dr} \cos(\theta_r) d\omega_r \\ &= \int_{\Omega} p_s R^2 d\omega_r + \int_{\Omega} p_d \left(\frac{R^2}{\pi} (A + B.K) \right) \cos(\theta_r) d\omega_r \\ &= p_s R^2 + p_d R^2 \\ &= (p_s + p_d) R^2 \end{aligned} \quad (8)$$

The condition $(p_s + p_d) \leq 1$ together with a plausible BRDF ensures that the energy conservation law and Helmholtz reciprocity are obeyed. Most diffuse BRDF models are dependent on the albedo of the surface. The albedo ρ is the reflectivity of the surface material. It is usually chosen using a best-fit approach [7]-[10]. A heuristic approach to estimate the albedo is based on the use of the Fresnel reflection coefficient R , where:

$$\rho = R^2 \quad (9)$$

The value of R is equal to the Fresnel reflection coefficient for a smooth plane. Hence the total energy available at the

surface for reflection purposes follows Fresnel theories, i.e. the energy that is not reflected is absorbed by the medium. In [5], reflection from rough surfaces is reduced by an attenuation factor. A reduction in reflection coefficient can be seen as a loss of energy through diffuse reflection. Therefore, the same attenuation factor can be implemented in the definitions of p_s and p_d in equations (2) and (3), such that:

$$p_s = e^{-(\Delta\Phi)^2} \quad (10)$$

$$p_d = 1 - p_s \quad (11)$$

$$\Delta\Phi = \frac{4\pi\Delta h \sin(\gamma)}{\lambda} \quad (12)$$

where γ is the incident grazing angle, Δh is the surface roughness and λ is the EM wavelength.

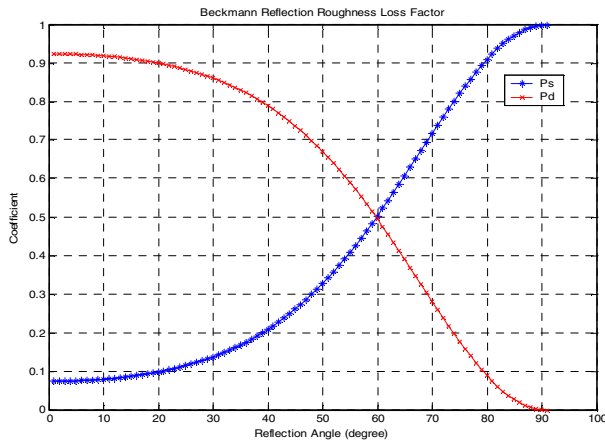


Figure 1. p_s and p_d for different reflection angles, frequency=1.92 GHz, $\Delta h = 0.02$

Given the surface roughness loss p_s defined previously, it can be seen from figure 1 that p_s is larger at smaller grazing angles and p_d is larger at near normal incidence. This agrees with the general understanding that diffuse scattering tends to be smaller when specular reflection is large.

The received power due to diffuse reflection (on a scattering surface) is now given by:

$$P_R = \frac{P_T G_T G_R \lambda^2}{(4\pi)^2 d_1^2 d_2^2} p_d \int_{\Omega_r} \cos(\theta_r) dA_s \quad (13)$$

and the received power due to specular reflection remains the same as in conventional ray tracing [1]-[3],[5]:

$$P_R = \frac{P_T G_T G_R \lambda^2}{(4\pi)^2 d_1^2 d_2^2} p_s R^2 \quad (14)$$

The hybrid scattering model satisfies both the energy conservation law and Helmholtz's reciprocity. It consists of specular reflection and diffuse reflection components. This is similar to other specular reflectance BRDF models used in computer graphics applications. The main difference is that for each surface/facet, the BRDF produces one reflected ray whereas the hybrid scattering model produces two reflected

rays (if the reflection law is met), i.e. a specular reflected ray and a diffuse reflected ray. The specular reflection used in the BRDF models is referred to as directional diffuse reflection, where a maximum peak reflection is generated at the specular reflection angle and its value gradually reduces as the viewing angle deviates. The specular reflection component in the hybrid scattering model is not directional diffuse and is considered as the coherent sum of the directional diffuse energy 'beam'. This energy 'beam' is then modelled using a GO ray.

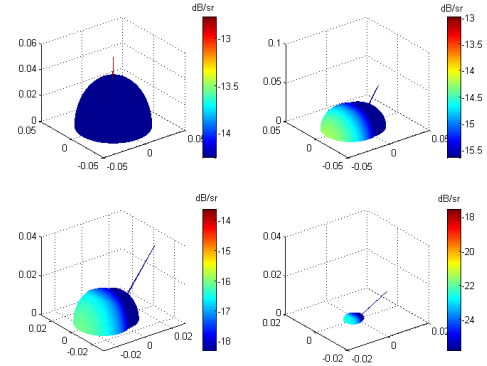


Figure 2a. Radiant intensity of the new hybrid reflectance model (dB/sr), clockwise from top left, $\theta_i = [0^\circ, -30^\circ, -45^\circ, -60^\circ]$, $p_s = 0.05$, $\sigma = 40^\circ$

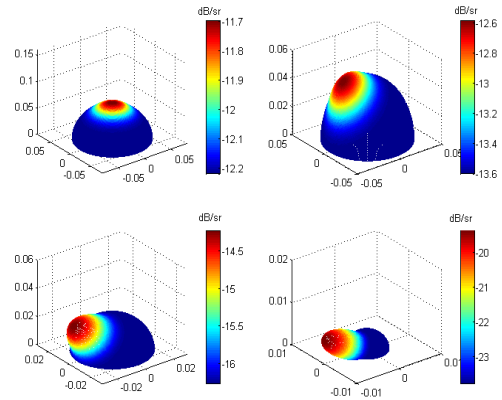


Figure 2b. Radiant intensity of the Phong model (dB/sr), clockwise from top left, $\theta_i = [0^\circ, 30^\circ, 45^\circ, 60^\circ]$, with $n=10$.

Figure 2a shows the radiant intensity for the hybrid scattering model, while Figure 2b shows the radiant intensity for a radiance Phong model [12]. The dimensions of the figures represent the 3D radial intensity.

One advantage of using a specular 'beam' compared to directional diffuse reflected rays is that the specular energy is higher and more focused in a 'beam' than in many individual diffuse reflection rays. As such, the computational cost is considerably lower when higher order propagation interactions are performed on a 'beam' (in the case of the hybrid and GO based ray tracing model) rather than many individual rays (in the case of the radiance model). Furthermore, as described in Section I, GO based propagation models have less computation effort when the same order of reflection is

considered, due to the lower number of interaction elements involved.

Scattering based models that use radiance may suffer from multipath resolution problems when the surfaces are partitioned into facets that are not small enough. In these radiance models, the total reflected radiant density (both specular and diffuse) is dependent on the reflecting surface area. This surface area dependency may result in an overestimate of the predicted power in radio propagation applications when surface/facet areas are large. However, if the resolution of the surface partitioning is increased, the computation cost is also increased. Hence, advanced techniques such as adaptive surface partitioning can be implemented to improve the processing efficiency [10]. In contrast, the GO based specular reflection approach can result in an underestimate of the predicted power since the surface area is not taken into consideration. However, this underestimation can be supplemented by the diffuse reflection in the hybrid scattering model. Thus, the hybrid GO and radiance based scattering model combines the powerful features of conventional GO reflection and scatter based models. The separation of specular reflection and diffuse reflection components, as in equations (13) and (14), also eases implementation in conventional ray tracing models (when implementing the effects of diffuse reflection).

III. COMPARISON WITH URBAN ROUTE MEASUREMENT

The hybrid scattering model has been implemented in an advanced three-dimensional site-specific microcellular ray tracing model [15]. The ray tracing model uses an image based approach to generate ray paths and operates in a 3D vectorized environment, which consists of buildings, foliage and terrain. Further description of the ray tracing model can be found in [15].



Figure 3. Trial map of city of Bristol

Predicted path loss and rms delay spread values are now compared with measured SIMO data at 1.92 GHz in a central Bristol location [16]. The basestation was mounted on a building top (approx. 30m from the ground) and 400 receiver points were placed along three routes as shown in Figure 3 (placed around 1.7m above the ground). An eight element ULA with $+45^\circ$ polarization was used at the basestation and a single omni-direction antenna was used at the mobile terminal.

A bandwidth of 20 MHz at a centre frequency of 1.92 GHz was used, with a frequency resolution of 156.25 kHz.

Three types of propagation model were used in this comparison study: 1) our ray tracing model using the newly proposed hybrid scattering model (referred to as ‘hybrid’); 2) the scattering based model described in [8] (referred to as ‘Eustace’); and 3) a conventional GO based ray tracing model (referred to as ‘GO’). For the ‘hybrid’ model, reflection was performed up to fourth order, diffraction up to second order and scattering up to first order. For the ‘Eustace’ model, a synthetic radar aperture technique was used to model the building and terrain scatter. This model was configured to consider vertical plane diffraction or single corner diffraction between the transmitter and receiver and the scattering terrain pixels. The ‘Eustace’ model operates using raster building and foliage data, rather than the original vector form. Diffraction is performed up to second order, while diffraction and scattering are performed up to second order. The conventional ‘GO’ model was implemented using the first model with the scattering features disabled.

Figure 4 shows a comparison of the path loss prediction for all three models compared to the actual measured data. A statistical summary of the absolute differences is given in Table 1. Figure 5 shows a comparison of the rms delay spread predictions and the resulting statistical summary of absolute differences is given in Table 2. The percentage values shown in brackets in Table 2 denote the difference in terms of the maximum measured rms delay spread (which was 910 ns).

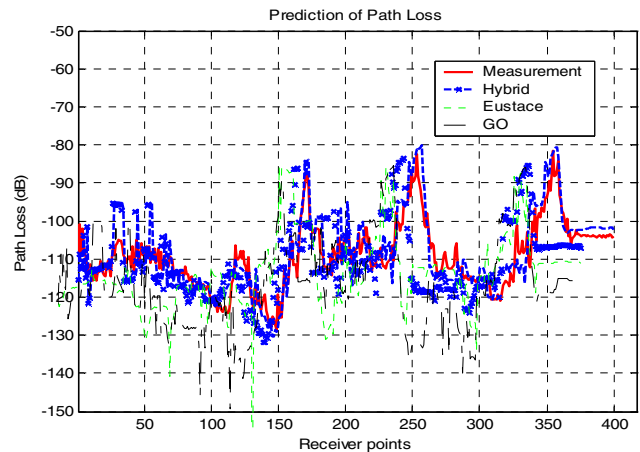


Figure 4. Comparison of path loss prediction.

TABLE 1. STATISTICAL SUMMARY OF PATH LOSS PREDICTION

Data Set	Mean Error (dB)	Std. Dev (dB)	Correlation
Hybrid	3.53	3.11	0.88
GO	5.15	4.81	0.86
Eustace	6.27	5.83	0.52

The results show that the new ‘hybrid’ ray tracer produces predictions that are significantly closer to the measurement data (compared to the ‘GO’ and ‘Eustace’ models). An improvement in mean path of around 1.6 dB and 2.7 dB was observed when compared to the ‘GO’ and ‘Eustace’ models respectively. A mean error improvement in the rms delay

spread predictions was also noted (around 2% and 5% of the maximum measured rms delay spread). As shown in Figures 3 and 4, for some parts of the measurement route, and especially towards the end, scattering (diffuse reflection) from buildings was seen to be significant. However, for large sections of the route, GO reflections dominate. An over prediction at around 30m into the route is due to a database error (line-of-sight error). Generally, the ‘Eustace’ scattering model does not perform as well as the ‘hybrid’ or ‘GO’ models, and this partly relates to its use of a rasterised database. It should also be noted that the ‘Eustace’ model is optimised for wide area coverage (up to 50km by 50km), and hence some accuracy is sacrificed in short-range predictions. Overall, the prediction accuracy is shown to improve significantly when hybrid scattering is applied.

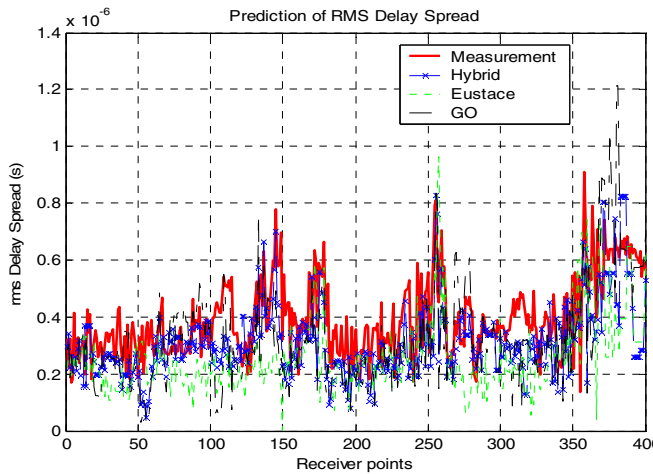


Figure 5. Comparison of rms. delay spread prediction.

TABLE 2. STATISTICAL SUMMARY OF RMS DELAY SPREAD PREDICTION

Data Set	Mean Error (ns)	Std. Dev. (ns)	Correlation
Hybrid	116.1 (12.7%)	90.58 (10%)	0.58
GO	131.5 (14.5%)	107.2 (11.8%)	0.54
Eustace	158.9 (17.5%)	108.4 (11.9%)	0.47

IV. CONCLUSIONS

In order to add diffuse reflection to a conventional GO based ray tracing model, a hybrid GO and radiance based scattering model was suggested. This new model combined all the advantages of conventional GO reflection and scatter-based models by modelling specular reflection using a GO Fresnel reflection coefficient and diffuse reflection using a diffuse reflectance radiance model. The hybrid model was shown to satisfy the required fundamental EM laws and could be implemented easily in existing GO based ray tracing models. A previous 3-D ray tracer was enhanced using the methods proposed and the prediction accuracy was analysed via comparison with measured data (and alternative modelling techniques). Comparisons with outdoor measurement data indicated that the hybrid model produced a significantly better level of agreement for path loss and rms delay spread. The work also indicated that for a number of locations, rough

surface scatter is a major component, even at frequencies as low as 1.92 GHz.

ACKNOWLEDGEMENTS

This work was part funded under the IST-2001-32549 ROMANTIK project. The authors would like to thank Prof. Mark Beach, Mythri Hunukumbure and Sze Ern Foo for the supply of measured data.

REFERENCES

- [1] G.E. Athanasiadou, A.R.Nix and J.P.McGeehan, “A microcellular ray-tracing propagation model and evaluation of its narrow-band and wide-band predictions,” *IEEE Journal on Selected Areas in Communications*, vol 18., No.3, pp.322- 335, March 2000.
- [2] T. Rautiainen, G. Wolffe and R. Hoppe, “Verifying Path Loss and Delay Spread Predictions of a 3D Ray Tracing Propagation Model in Urban Environments,” in *56th IEEE Vehicular Tech. Conference*, Sept 2002.
- [3] G. Liang and H. L. Bertoni, “A New Approach to 3-D Ray Tracing for Propagation Prediction in Cities,” *IEEE Trans. Antennas Propagat.*, Vol. 46, 1998.
- [4] D.A.McNamara, C.W.I.Pistorius, and J.A.G.Malherbe, *Introduction to the Uniform Geometrical Theory of Diffraction*. Norwood, MA:Artech House, 1990.
- [5] R.J.Luebbers, “A heuristic UTD slope diffraction coefficient for rough lossy wedges,” *IEEE Trans. on Ant. and Prop.*, vol.37, no.2, Feb 1989.
- [6] P.Beckmann and A.Spizzichino, *The scattering of electromagnetic waves from rough surfaces*, Pergamon Press, 1963.
- [7] T.Brook, P.F.Driessen, R.L.Kirilin, “Propagation measurements using synthetic aperture radar techniques”, *Vehicular Technology Conference 1996*, IEEE 46th,vol 3, pp. 1633 – 1637, 28 April-1 May 1996.
- [8] E.K.Tameh, A.R.Nix, and M.A.Beach, “3D integrated macro and microcellular propagation model, based on the use of photogrammetric terrain and building data,” in *IEEE Veh. Tech. Conf.*, Phoenix, AZ, May 1997.
- [9] C. Kloch, G. Liang, J. B. Anderson, G. F. Pedersen and H. L. Bertoni, “Comparison of Measured and Predicted Time Dispersion and Direction of Arrival for Multipath in a Small Cell Environment,” *IEEE Trans. on Antennas and Propagat.*, Vol. 49, No. 9, Sept 2001.
- [10] E.Montiel, A.S.Aguado and F.X.Sillion, “A Radiance Model for Predicting Radio Wave Propagation in Irregular Dense Urban Ares,” *IEEE Trans. on Ant. and Prog.*, vol.51, no.11, Nov, 2003.
- [11] E.F.Knott, J.F.Shaeffler and M.T.Tuley, *Radar Cross Section*, Aztech House (US), 1985.
- [12] R.Lewis, “Making shaders more physically plausible,” *Eurographics*,’94, vol.13, no.3, pp.1-13, 1994.
- [13] H. E. Rushmeier and K. Torrance, “Extending the Radiosity Method to Include Specular Reflecting and Translucent Materials,” *ACM Trans. on Graphics*, Vol. 9, No. 1, Jan 1990.
- [14] M.Oren and S.K.Nayar, “Generalization of the Lambertian model and implications for machine vision,” *International Journal of Computer Vision*, Feb, 1994.
- [15] K. H. Ng, E. Tameh and A. R. Nix, “An Advanced Multi-Element Microcellular Ray Tracing Model,” in *Proc. of 1st International Symposium on Wireless Communication Systems 2004*, to be published.
- [16] S. E. Foo, M. A. Beach, P. Karlsson, P. Eneroth, B. Lindmark and J. Johansson, Spatio-Temporal Investigation of UTRA FDD Channels. *Proc. IEE 3G Mobile Communication Technologies 2002*, pp. 175–179.